

## Calculation of Multichannel Reactions in the Four-Nucleon System above Breakup Threshold

A. Deltuva<sup>1,2</sup> and A. C. Fonseca<sup>1</sup>

<sup>1</sup>*Centro de Física Nuclear, Universidade de Lisboa, P-1649-003 Lisboa, Portugal*

<sup>2</sup>*Institute of Theoretical Physics and Astronomy, Vilnius University, A. Goštauto 12, LT-01108 Vilnius, Lithuania*

(Received 16 June 2014; published 5 September 2014)

The exact four-body equations of Alt, Grassberger, and Sandhas are solved for neutron-<sup>3</sup>He and proton-<sup>3</sup>H scattering in the energy regime above the four-nucleon breakup threshold. Cross sections and spin observables for elastic, transfer, charge-exchange, and breakup reactions are calculated using realistic nucleon-nucleon interaction models, including the one with effective many-nucleon forces due to explicit  $\Delta$ -isobar excitation. The experimental data are described reasonably well with only few exceptions such as vector analyzing powers.

DOI: 10.1103/PhysRevLett.113.102502

PACS numbers: 21.45.-v, 21.30.-x, 24.70.+s, 25.10.+s

Collisions and reactions are among the most important processes used to study various quantum systems ranging from ultracold atoms to nuclear and particle physics. However, reliable information about their properties can be extracted from experimental data only when an accurate theoretical description of the scattering process is available, which is much more complicated to obtain as compared to that of bound systems. With the three-particle system already well under control, the next step is the study of collisions and reactions involving four particles.

Because of its inherent complexity, rich structure of resonances, and multitude of channels, the four-nucleon ( $4N$ ) system constitutes a highly challenging but also promising theoretical laboratory to test the nucleon-nucleon ( $NN$ ) force models. But for that to be possible, one needs to be able to solve numerically, over a broad range of energy, the corresponding scattering equations in momentum or coordinate space. Work on this problem evolved slowly over the years but took a fast leap forward in the last 10 years.

Four-nucleon scattering results with realistic force models emerged first through coordinate space calculations but were limited to single channel  $n$ -<sup>3</sup>H and  $p$ -<sup>3</sup>He [1–3] and  $p$ -<sup>3</sup>H [4] reactions below inelastic threshold. In that region, the  $4N$  system exhibits a rich structure of resonances [5] in different partial waves that have been well identified in the literature and whose understanding in terms of the underlying force models constitutes a major yet unresolved challenge for theory. More recent results show that adding a three-nucleon ( $3N$ ) force does not necessarily improve the agreement with the experimental data [3,6,7], unless particular  $3N$  force models are used [8]. As in the three-nucleon system, complex scaling methods are now being used to calculate single channel reactions above breakup threshold, however, with semirealistic  $S$ -wave interactions so far [9].

Given that the treatment of the Coulomb interaction between protons became possible in momentum-space

calculations by using the method of screening and renormalization [10], solutions of the Alt, Grassberger, and Sandhas (AGS) equations [11] for the transition operators have been accomplished at energies below breakup threshold for a number of realistic  $NN$  interactions [12]. Because asymptotic boundary conditions are naturally imposed by the way one handles the two-cluster singularities, one could calculate cross sections and spin observables for all two-cluster reactions ranging from  $n$ -<sup>3</sup>H [12],  $p$ -<sup>3</sup>He [13],  $n$ -<sup>3</sup>He,  $p$ -<sup>3</sup>H, and  $d$ - $d$  [14] elastic scattering to rearrangement reactions such as <sup>3</sup>H( $p, n$ )<sup>3</sup>He, <sup>2</sup>H( $d, p$ )<sup>3</sup>H, and <sup>2</sup>H( $d, n$ )<sup>3</sup>He [14] and their respective time reversal. In this energy range, calculations were done using real-axis integration with subtraction method, spline interpolation, and Padé summation [15] for matrix elements of the transition operators [12]. This approach was extended to allow for an explicit  $\Delta$ -isobar excitation yielding effective  $3N$  and  $4N$  forces [16]. Unlike coordinate space methods, adding an irreducible  $3N$  force constitutes a major stumbling block for momentum-space calculations that has not yet been resolved, except for bound state calculations [17].

Given the complex analytical structure of the four-body kernel in momentum space above three- and, especially, four-cluster threshold, going beyond breakup threshold seemed for a while an impossible endeavor. Using complex energy in the form of  $Z = E + i\epsilon$ , where  $\epsilon$  is a finite quantity [18], was a mirage that only worked well when a new integration method with special weights [19] was developed, taking into account the presence of the quasi-singularities. This enabled fully realistic state-of-the-art calculations of  $n$ -<sup>3</sup>H [19] and  $p$ -<sup>3</sup>He [20] elastic scattering up to 35 MeV nucleon energy.

In this Letter, we present the most challenging step in  $4N$  scattering research by addressing  $n$ -<sup>3</sup>He and  $p$ -<sup>3</sup>H mixed isospin  $T = 0$  and 1 reactions above the breakup threshold where the singularity structure of the four-nucleon kernel attains its highest complexity due to a variety of open

channels. This continues the investigations we pioneered years ago below breakup [14]. Because all two-, three-, and four-cluster channels are open, we are confronted with the most complex nuclear reaction calculation to date that actually resembles a typical nuclear reaction process where elastic, charge exchange, transfer, and breakup take place simultaneously.

We use the symmetrized AGS equations [12] as appropriate for the four-nucleon system in the isospin formalism. They are integral equations for the four-particle transition operators  $\mathcal{U}_{\beta\alpha}$ , i.e.,

$$\mathcal{U}_{11} = -(G_0 t G_0)^{-1} P_{34} - P_{34} U_1 G_0 t G_0 \mathcal{U}_{11} + U_2 G_0 t G_0 \mathcal{U}_{21}, \quad (1a)$$

$$\mathcal{U}_{21} = (G_0 t G_0)^{-1} (1 - P_{34}) + (1 - P_{34}) U_1 G_0 t G_0 \mathcal{U}_{11}. \quad (1b)$$

Here,  $\alpha = 1$  corresponds to the 3 + 1 partition (12,3)4 whereas  $\alpha = 2$  corresponds to the 2 + 2 partition (12)(34); there are no other distinct two-cluster partitions in the system of four identical particles. The symmetrized 3 + 1 or 2 + 2 subsystem transition operators are obtained from the respective integral equations

$$U_\alpha = P_\alpha G_0^{-1} + P_\alpha t G_0 U_\alpha. \quad (2)$$

The free resolvent at the complex energy  $E + i\epsilon$  is given by

$$G_0 = (E + i\epsilon - H_0)^{-1}, \quad (3)$$

with  $H_0$  being the free Hamiltonian. The pair (12) transition matrix

$$t = v + v G_0 t \quad (4)$$

is derived from the potential  $v$ ; for the  $pp$  pair  $v$  includes both the nuclear and the screened Coulomb potential. Thereby all transition operators acquire parametric dependence on the screening radius  $R$ , but for simplicity it is suppressed in our notation. The full antisymmetry of the four-nucleon system is ensured by the permutation operators  $P_{ab}$  of particles  $a$  and  $b$  with  $P_1 = P_{12}P_{23} + P_{13}P_{23}$  and  $P_2 = P_{13}P_{24}$ , together with the special symmetry of basis states as pointed out in Refs. [12,19].

The numerical calculations are performed for complex energies, i.e., with finite  $\epsilon$ . A special integration method developed in Ref. [19] is used to treat the quasisingularities of the AGS equations (1). The limit  $\epsilon \rightarrow +0$  needed for the calculation of scattering amplitudes and observables is obtained by the extrapolation of finite  $\epsilon$  results. Beside the point method proposed in Ref. [21] and applied in Refs. [18,19] we use, as an additional accuracy check, cubic spline extrapolation with nonstandard choice of the boundary conditions, namely, the one ensuring continuity

of the third derivative [22]. These two different methods lead to indistinguishable results confirming the reliability of the calculations. We use  $\epsilon$  ranging from 1 to 2 MeV at the lowest considered energies and from 2 to 4 MeV at the highest considered energies. About 30 grid points for the discretization of each momentum variable are used.

The limit  $\epsilon \rightarrow +0$  is calculated separately for each value of the Coulomb screening radius  $R$ . After that, the renormalization procedure is performed as described in Refs. [10,13,14] and the results are checked to be independent of  $R$  provided  $R$  is large enough. In the present calculations, we found  $R$  ranging from 10 to 16 fm (depending on reaction and energy) to be fully sufficient for convergence.

The results are also fully converged with respect to the partial-wave expansion. The calculations include  $2N$  partial waves with orbital angular momentum  $l_x \leq 5$ ,  $3N$  partial waves with spectator orbital angular momentum  $l_y \leq 5$  and total angular momentum  $J_y \leq \frac{11}{2}$ ,  $4N$  partial waves with 1 + 3 and 2 + 2 orbital angular momentum  $l_z \leq 6$ , resulting in up to about 21 000 channels for fixed  $4N$  total angular momentum and parity. For some reactions, e.g.,  $n$ - $^3\text{He}$  elastic scattering, the partial-wave convergence is considerably faster, allowing for a reduction in the employed angular momentum cutoffs. After the AGS equations are solved, for the calculation of observables it is sufficient to include only the initial and final 1 + 3 states with  $l_z \leq 5$  or even  $l_z \leq 4$ , the only exception being the transfer reactions requiring  $l_z \leq 6$  for both 1 + 3 and 2 + 2 channels. Further technical details on the solution of the four-nucleon AGS equations can be found in Refs. [12,19].

We study  $n$ - $^3\text{He}$  and  $p$ - $^3\text{H}$  scattering using realistic high-precision two-baryon potentials, namely, the purely nucleonic inside-nonlocal outside-Yukawa (INOY04) potential by Doleschall [3,23] and the coupled-channel extension of the charge-dependent Bonn potential (CD Bonn) [24], called CD Bonn +  $\Delta$  [25]. The latter allows for an excitation of a nucleon to a  $\Delta$  isobar effectively yielding three- and four-nucleon forces (3NF and 4NF). The  $^3\text{He}$  ( $^3\text{H}$ ) binding energy calculated with CD Bonn +  $\Delta$  and INOY04 potentials is 7.53 (8.28) and 7.73 (8.49) MeV, respectively; the experimental value is 7.72 (8.48) MeV. Therefore, most of our predictions are obtained using INOY04 as it nearly reproduces the experimental binding energies. The calculations with CD Bonn +  $\Delta$  are done at fewer selected energies. Thus, we will compare results obtained with a pure nucleonic pairwise interaction that by itself alone leads to the correct  $^3\text{He}$  and  $^3\text{H}$  binding, with those obtained with a force model where effective  $3N$  and  $4N$  forces are present but that does not quite reproduce the three-nucleon binding.

In Fig. 1 we show the  $n$ - $^3\text{He}$  total and partial cross sections for all open channels as functions of the incoming neutron beam energy  $E_n$  ranging from 0 to 24 MeV. Results obtained using the INOY04 potential are compared with

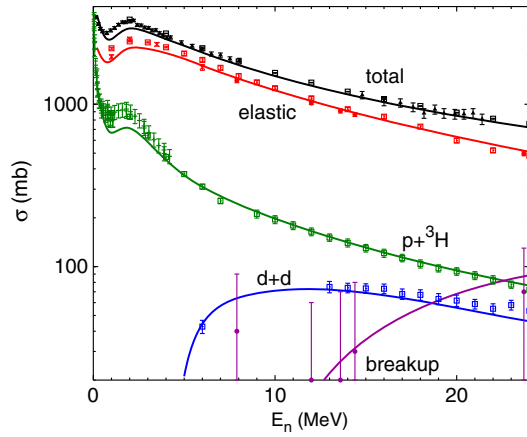


FIG. 1 (color online).  $n$ - ${}^3\text{He}$  total and partial cross sections as functions of the neutron beam energy calculated using INOY04 potential. The data are from Refs. [26–30].

data from Refs. [26–30]. Below 5 MeV where several resonant  $4N$  states are present, the theory underpredicts the data as already pointed out in Ref. [14], but at higher energies the predictions follow the data, not just for the largest total and elastic cross sections but also for the  ${}^3\text{He}(n, p){}^3\text{H}$  charge exchange and the  ${}^3\text{He}(n, d){}^2\text{H}$  transfer reactions. Using unitarity we calculate also the total breakup cross section (three plus four cluster), which rises fast and quickly becomes the dominant inelastic channel; the few existing data points have large error bars and, except for the first one at  $E_n = 8$  MeV, are consistent with our predictions.

In Figs. 2 and 3 we show the angular dependence of the differential cross sections  $d\sigma/d\Omega$  and nucleon analyzing powers  $A_y$  for  $n$ - ${}^3\text{He}$  and  $p$ - ${}^3\text{H}$  elastic scattering at a few selected energies above the four-cluster breakup threshold. Differential cross sections peak at forward direction and

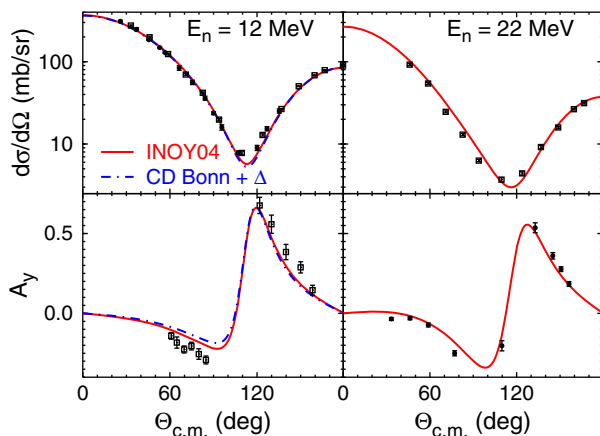


FIG. 2 (color online). Differential cross section and neutron analyzing power of elastic  $n$ - ${}^3\text{He}$  scattering at 12 and 22 MeV neutron energy. Results obtained with potentials INOY04 (solid curves) and CD Bonn +  $\Delta$  (dashed-dotted curves) are compared with data from Refs. [28,31–33].

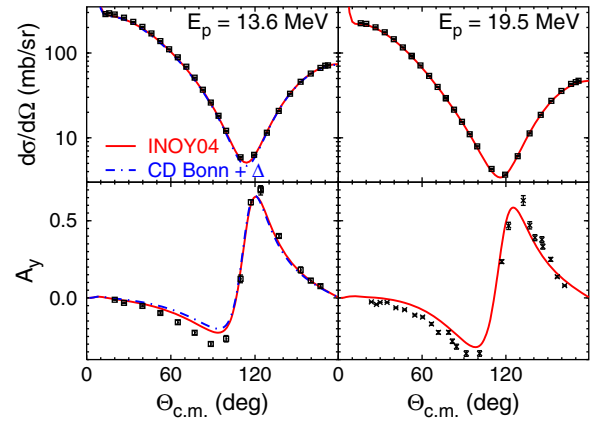


FIG. 3 (color online). Differential cross section and proton analyzing power of elastic  $p$ - ${}^3\text{H}$  scattering at 13.6 and 19.5 MeV proton energy. Curves as in Fig. 2. The data are from Refs. [34,35].

show a deep minimum around  $\Theta_{\text{c.m.}} = 115^\circ$ . Unlike at low energies, analyzing powers develop a shallow minimum around  $90^\circ$  before they rise to a maximum around  $120^\circ$ . All these special features in the observables slowly move to larger angles with increasing energy. Much like in  $p$ - $d$  and  $p$ - ${}^3\text{He}$  elastic scattering, we observe that a reasonable description of the data [28,31–35] emerges as the energy rises; there remain only small or at most moderate discrepancies, the most notable one being around the  $A_y$  minimum. At  $E_n = 12$  MeV and  $E_p = 13.6$  MeV, we show also the results obtained with the CD Bonn +  $\Delta$  interaction where effective  $3N$  and  $4N$  forces are included. The difference between the INOY04 and CD Bonn +  $\Delta$  only shows up around the minima of  $d\sigma/d\Omega$  and  $A_y$ , indicating that the elastic scattering results are not very sensitive to the force model.

Next we consider the charge exchange reaction  ${}^3\text{H}(p, n){}^3\text{He}$  at proton beam energy  $E_p$  ranging from 7

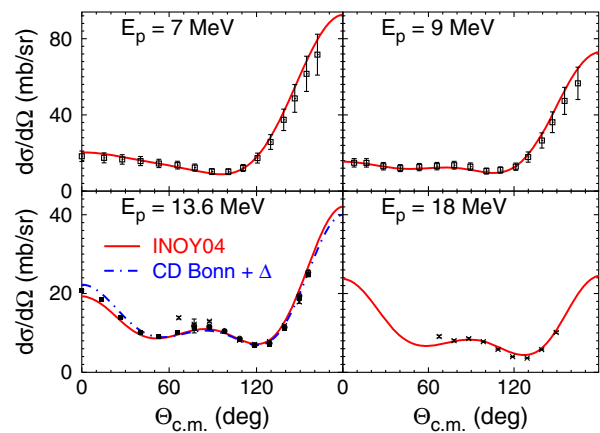


FIG. 4 (color online). Differential cross section of  ${}^3\text{H}(p, n){}^3\text{He}$  reaction at 7, 9, 13.6, and 18 MeV proton energy. Curves as in Fig. 2. The data are from Refs. [36–39].

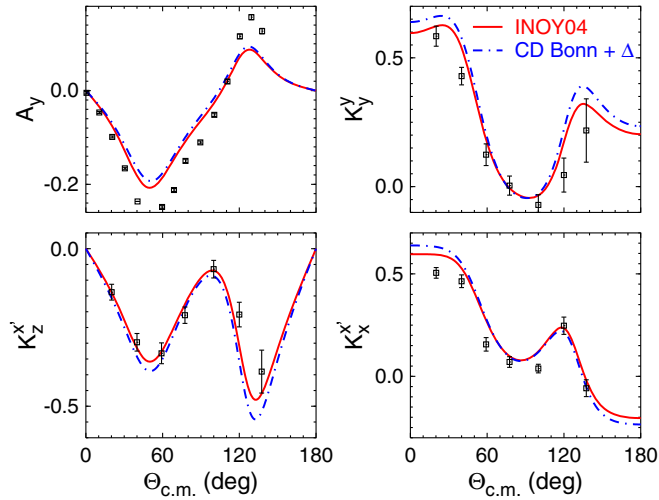


FIG. 5 (color online). Proton analyzing power and proton to neutron polarization transfer coefficients of  ${}^3\text{H}(p, n){}^3\text{He}$  reaction at 13.6 MeV proton energy. Curves as in Fig. 2. The data are from Refs. [40,41].

to 18 MeV. In contrast to elastic scattering, the differential cross section for the charge-exchange reaction exhibits a strong energy dependence as demonstrated in Fig. 4. In particular, a simple shape of  $d\sigma/d\Omega$  at  $E_p = 7$  MeV with a single minimum around  $\Theta_{\text{c.m.}} = 95^\circ$  evolves into a more complex one with a local maximum around  $80^\circ$ – $90^\circ$  and two minima near  $50^\circ$  and  $120^\circ$ . Furthermore, the backward peak decreases rapidly with increasing energy while the evolution of the forward peak is nonmonotonic: first it slowly decreases but then starts to increase for  $E_p > 10$  MeV. Given such a complicated behavior of the differential cross section for the charge-exchange reaction, the observed good agreement between our theoretical predictions and experimental data from Refs. [36–39] is very impressive. In addition to INOY04 predictions, at  $E_p = 13.6$  MeV we show the results obtained using the CD Bonn +  $\Delta$  interaction model. We find differences of about 10% and 5% at forward and backward angles, respectively. Differences between INOY04 and CD Bonn +  $\Delta$  become even more pronounced in the spin observables, reaching up to 10%–15%. In Fig. 5 we show proton analyzing power  $A_y$  and proton to neutron polarization transfer coefficients  $K_y'$ ,  $K_z'$ , and  $K_x'$  for the charge exchange reaction at  $E_p = 13.6$  MeV. The shape of the observables with several extrema is reproduced by both interaction models, but INOY04 yields a better quantitative description of the data [40,41], especially for the polarization transfer coefficients. The extrema of  $A_y$  represent the worst case with a significant discrepancy between theory and experiment. Otherwise, the overall description of the data is impressive given its complexity and the absence of any adjustable parameter in the calculations or the interactions after they have been fit to the  $NN$  data.

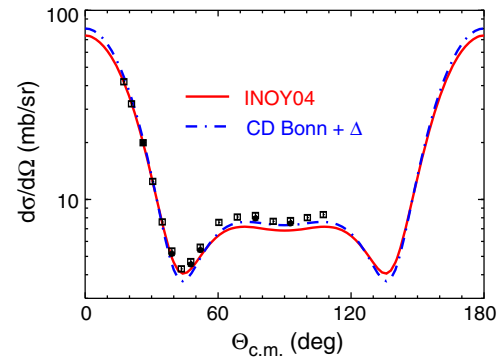


FIG. 6 (color online). Differential cross section of  ${}^3\text{H}(p, d){}^2\text{H}$  reaction at 13.6 MeV proton lab energy. Curves as in Fig. 2. The data are from Refs. [34,42].

Finally in Fig. 6 we show the differential cross section for the  ${}^3\text{H}(p, d){}^2\text{H}$  transfer reaction at  $E_p = 13.6$  MeV. The shape of the observable having several local extrema and a forward peak is well reproduced by calculations except at larger angles  $\Theta_{\text{c.m.}} > 45^\circ$  where, after the minimum, the data [34,42] are slightly underpredicted. The sensitivity to the force model reaches 10%, but this time the CD Bonn +  $\Delta$  interaction model provides a better description of the data around  $\Theta_{\text{c.m.}} = 90^\circ$ . This sensitivity to some extent may be caused by the correlation with  ${}^3\text{H}$  binding energy, as found in Ref. [43] for  ${}^2\text{H}(d, p){}^3\text{H}$  fusion below three-cluster threshold.

In summary, the most advanced state-of-the-art calculations involving all multichannel reactions in the four-nucleon system have been performed above breakup threshold using exact AGS equations. The results were obtained for mixed isospin ( $T = 0$  and 1) reactions initiated by the scattering of a neutron on a  ${}^3\text{He}$  target or a proton on a  ${}^3\text{H}$  target. Realistic nuclear force models INOY04 and CD Bonn +  $\Delta$ , the latter yielding also effective many-nucleon forces due to  $\Delta$ -isobar excitation, were used together with the proton-proton Coulomb interaction included via the screening and renormalization method. Calculations are fully converged with respect to numerical integration, angular momentum decomposition, and Coulomb screening.

The results are in good agreement with the experimental data except for few observables in specific angular regions. Even in such cases, the overall reproduction of the complex structure of the observables having several local extrema is impressive as demonstrated, e.g., for differential cross section and polarization transfer coefficients in the  ${}^3\text{H}(p, n){}^3\text{He}$  reaction. The only sizable discrepancy is found for proton analyzing power in the charge-exchange reaction. Calculations with different potentials show that inelastic reactions and spin observables are more sensitive to interaction models.

Further calculations, including elastic, transfer, and breakup reactions in deuteron-deuteron scattering, are

under way to gain deeper insight into the four-nucleon system and the chosen nuclear force models. This work also opens the door to study the validity of approximate methods in reaction theory to treat direct nuclear reactions. Furthermore, the present developments are also of great importance to cold-atom physics where the momentum-space AGS equations were proven to be a powerful tool to study universal phenomena [44,45]. For example, implementing the ideas of this work in the calculations of Ref. [46] will enable the description of four-atom recombination at finite temperature.

- 
- [1] M. Viviani, A. Kievsky, S. Rosati, E. A. George, and L. D. Knutson, *Phys. Rev. Lett.* **86**, 3739 (2001).
- [2] A. Kievsky, S. Rosati, M. Viviani, L. E. Marcucci, and L. Girlanda, *J. Phys. G* **35**, 063101 (2008).
- [3] R. Lazauskas and J. Carbonell, *Phys. Rev. C* **70**, 044002 (2004).
- [4] R. Lazauskas, *Phys. Rev. C* **79**, 054007 (2009).
- [5] D. R. Tilley, H. Weller, and G. M. Hale, *Nucl. Phys. A* **541**, 1 (1992).
- [6] R. Lazauskas, J. Carbonell, A. Fonseca, M. Viviani, A. Kievsky, and S. Rosati, *Phys. Rev. C* **71**, 034004 (2005).
- [7] B. Fisher, C. Brune, H. Karwowski, D. Leonard, E. Ludwig, T. Black, M. Viviani, A. Kievsky, and S. Rosati, *Phys. Rev. C* **74**, 034001 (2006).
- [8] M. Viviani, L. Girlanda, A. Kievsky, and L. E. Marcucci, *Phys. Rev. Lett.* **111**, 172302 (2013).
- [9] R. Lazauskas, *Phys. Rev. C* **86**, 044002 (2012).
- [10] A. Deltuva, A. C. Fonseca, and P. U. Sauer, *Phys. Rev. C* **71**, 054005 (2005).
- [11] P. Grassberger and W. Sandhas, *Nucl. Phys.* **B2**, 181 (1967); E. O. Alt, P. Grassberger, and W. Sandhas, JINR report No. E4-6688, 1972.
- [12] A. Deltuva and A. C. Fonseca, *Phys. Rev. C* **75**, 014005 (2007).
- [13] A. Deltuva and A. C. Fonseca, *Phys. Rev. Lett.* **98**, 162502 (2007).
- [14] A. Deltuva and A. C. Fonseca, *Phys. Rev. C* **76**, 021001(R) (2007).
- [15] G. A. Baker, *Essentials of Padé Approximants* (Academic Press, New York, 1975).
- [16] A. Deltuva, A. C. Fonseca, and P. U. Sauer, *Phys. Lett. B* **660**, 471 (2008).
- [17] A. Nogga, H. Kamada, W. Glöckle, and B. R. Barrett, *Phys. Rev. C* **65**, 054003 (2002).
- [18] E. Uzu, H. Kamada, and Y. Koike, *Phys. Rev. C* **68**, 061001(R) (2003).
- [19] A. Deltuva and A. C. Fonseca, *Phys. Rev. C* **86**, 011001(R) (2012).
- [20] A. Deltuva and A. C. Fonseca, *Phys. Rev. C* **87**, 054002 (2013).
- [21] L. Schlessinger, *Phys. Rev.* **167**, 1411 (1968).
- [22] K. Chmielewski, A. Deltuva, A. C. Fonseca, S. Nemoto, and P. U. Sauer, *Phys. Rev. C* **67**, 014002 (2003).
- [23] P. Doleschall, *Phys. Rev. C* **69**, 054001 (2004).
- [24] R. Machleidt, *Phys. Rev. C* **63**, 024001 (2001).
- [25] A. Deltuva, R. Machleidt, and P. U. Sauer, *Phys. Rev. C* **68**, 024005 (2003).
- [26] M. E. Battat *et al.*, *Nucl. Phys.* **12**, 291 (1959).
- [27] B. Haesner, W. Heeringa, H. Klages, H. Dobiasch, G. Schmalz, P. Schwarz, J. Wilczynski, B. Zeitnitz, and F. Käppeler, *Phys. Rev. C* **28**, 995 (1983).
- [28] M. Drosig, D. McDaniel, J. Hopkins, J. Seagrave, R. Sherman, and E. Kerr, *Phys. Rev. C* **9**, 179 (1974).
- [29] J. D. Seagrave, L. Cranberg, and J. E. Simmons, *Phys. Rev.* **119**, 1981 (1960).
- [30] J. H. Gibbons and R. L. Macklin, *Phys. Rev.* **114**, 571 (1959).
- [31] B. Haesner *et al.*, in *EXFOR Database* (NNDC, Brookhaven, 1982).
- [32] P. W. Lisowski, T. C. Rhea, R. L. Walter, C. E. Busch, and T. B. Clegg, *Nucl. Phys.* **A259**, 61 (1976).
- [33] H. O. Klages, W. Heeringa, H. Dobiasch, B. Fischer, B. Haesner, P. Schwarz, J. Wilczynski, and B. Zeitnitz, *Nucl. Phys.* **A443**, 237 (1985).
- [34] J. L. Detch, R. L. Hutson, N. Jarmie, and J. H. Jett, *Phys. Rev. C* **4**, 52 (1971).
- [35] R. Darves-Blanc, N. Van Sen, J. Arvieux, A. Fiore, J. C. Gondrand, and G. Perrin, *Lett. Nuovo Cimento* **4**, 16 (1972).
- [36] W. E. Wilson, R. L. Walter, and D. B. Fossan, *Nucl. Phys.* **27**, 421 (1961).
- [37] M. Drosig, *Nucl. Sci. Eng.* **67**, 190 (1978); in *EXFOR Database* (NNDC, Brookhaven, 1978).
- [38] N. Jarmie and J. H. Jett, *Phys. Rev. C* **16**, 15 (1977).
- [39] R. Allas, L. Beach, R. Bondelid, E. Diener, E. Petersen, J. Lambert, P. Treado, and I. Šlaus, *Phys. Rev. C* **9**, 787 (1974).
- [40] J. Jarmer, R. Haight, J. Simmons, J. Martin, and T. Donoghue, *Phys. Rev. C* **9**, 1292 (1974).
- [41] R. C. Haight, J. E. Simmons, and T. R. Donoghue, *Phys. Rev. C* **5**, 1826 (1972).
- [42] N. Jarmie and J. H. Jett, *Phys. Rev. C* **10**, 54 (1974).
- [43] A. Deltuva and A. C. Fonseca, *Phys. Rev. C* **81**, 054002 (2010).
- [44] A. Deltuva, *Phys. Rev. A* **82**, 040701(R) (2010).
- [45] A. Deltuva, *Europhys. Lett.* **95**, 43002 (2011).
- [46] A. Deltuva, *Phys. Rev. A* **85**, 012708 (2012).